Acetone and Ethanol Extraction from Water by Means of Membrane: Modeling and Numerical Simulation

[1]*Mahmoud Reza Sohrabi,* [2]*Azam Marjani,* [2]*Saeed Shirazian and* [3]*Sadegh Moradi*

[1]Department of Chemistry, North Tehran Branch, Islamic Azad University-Tehran-Iran
[2]Department of Chemistry, Arak Branch, Islamic Azad University-Arak-Iran
[3]Department of Chemical Engineering, Faculty of Engineering,
Arak University, Arak 38156-8-8349, Iran

Abstract: This study presents mass transfer modeling of solvent extraction by membrane contactors. The extraction system was a membrane contactor, an aqueous solution of ethanol and acetone as the feed and a near-critical phase of carbon dioxide as the solvent. Model was based on solving conservation equations for solutes in the membrane contactor. The equations of the model were solved by numerical method based on finite element method (FEM). The simulation results for ethanol and acetone showed an average deviation of 15.6% and 2.5% with the experimental data, respectively. Simulation results for the extraction of acetone are more accurate than those for ethanol mostly due to a better estimation of the transport properties. The developed mass transfer model is more accurate than other models and represents a general approach for simulation of membrane contactors.

Key words: Membrane contactor · Acetone · Ethanol · Separation · Numerical simulation

INTRODUCTION

Separation processes using membrane contactors have been conducted in concentration or purification processes such as solvent extraction, gas absorption, ion exchange and membrane distillation. In membrane contactors, the membrane mainly operates as a physical barrier between two fluids and unlike most membrane operations, the membrane has no selectivity to the separation, i.e., it has no impact on the partition coefficients [1-4].

Among the membrane modules available as membrane contactors, hollow-fiber membrane contactors (HFMCs) have attracted many attentions. These devices provide high surface/volume ratio for mass transfer and separation. These contactors offer some advantages compared with conventional contactors such as dispersion columns [1]. In HFMCs, the interfacial mass-transfer area is much higher and better controlled, whereas the hydrophilic or hydrophobic nature of the membrane determines the position of the interface between the feed and the solvent. Meanwhile, these contactors allow the possibility to immobilize this interface at the pore's mouth by applying an adequate

trans-membrane pressure gradient. Therefore, the main advantage of membrane contactors is that they allow a dispersion-free contact, so emulsions cannot be formed during the separation process. In addition, the velocities of both phases can be chosen independently and , as a result neither flooding nor foaming problems arise [5-9].

One of the applications of membrane contactors is supercritical extraction. This process is called porocritical extraction. Porocritical process or porocritical extraction is a commercial supercritical fluid extraction (SFE) which utilizes a hollow-fiber membrane contactor (HFMC) [4]. In this process a macroporous membrane allows contact between two phases. The aqueous feed solution is passed on one side, while the extraction solvent, which is a near-critical or a super-critical fluid, is flowed on the other side. Where the applied membrane is hydrophobic, i.e. the aqueous solution does not wet the membrane pores. The chemical potential gradient that generates a mass transfer through the membrane is due to the concentration gradient of the solute between the two phases. In porocritical extraction, there are four steps for the transfer of a solute across the membrane: transport through the boundary layer of the liquid feed solution; solubilization in the near-critical or SCF extraction phase;

Corresponding Author: Azam Marjani, Faculty member of Islamic Azad University-Arak Branch, E-mail: a-marjani@iau-arak.ac.ir
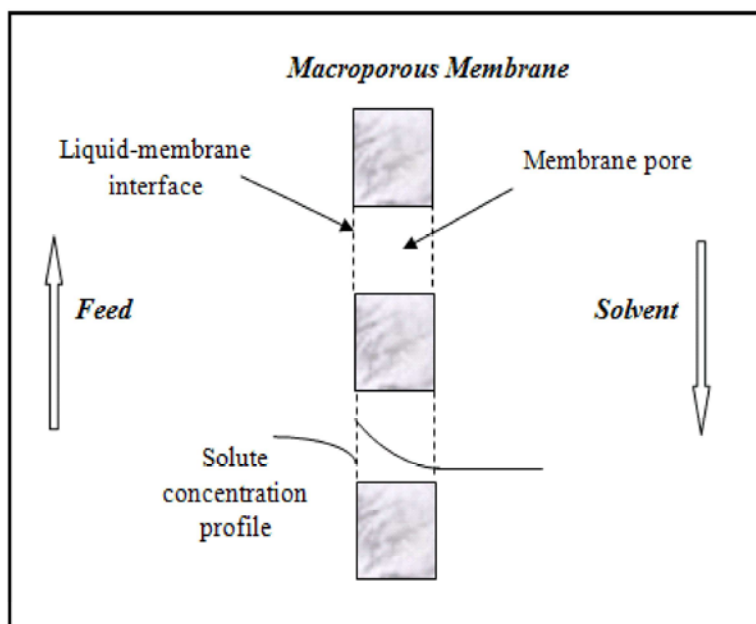
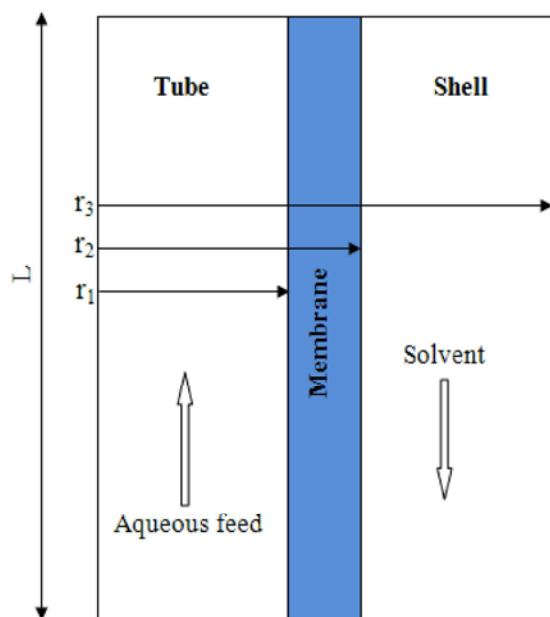Fig. 1: Principles of mass transfer in porocritical extraction [4]

Fig. 2: Model domain

diffusion through the stagnant extraction phase within the pores; transport through the boundary layer of the extraction phase. Fig. 1 schematically shows the principles of this process [4].

The main objective of this study is to develop and solve a mass transfer model for the prediction of porocritical process. The developed model considers both axial and radial diffusions in the tube, membrane and shell

compartments of the contactor. It also considers the convection in both of the tube and shell sides. The model has been finally validated using experimental data reported by Bothun *et al.* [10] for the extraction of ethanol and acetone from aqueous solutions.

Model Development: In order to validate the simulation results, experimental data reported by Bothun *et al.* [10] for the extraction of ethanol and acetone from aqueous solutions were used. The contactor consists of a single hollow fiber housed in a stainless steel tube. The liquid feed (aqueous solution) is flowed inside the fiber and the solvent (near-critical CO_2) is passed countercurrent-wise outside the fiber. The simulations were carried out at identical conditions employed in conducting experiments.

Formulation of Mass Transfer: The conservation equations for the solute in the contactor were derived and solved to predict the performance of the contactor. The model is developed for a hollow fiber, as shown in Fig. 2, through which the liquid flows with a fully developed laminar parabolic velocity profile. The fiber is surrounded by the solvent gas which flows in a laminar mode in the opposite direction of the feed stream. Therefore, the membrane contactor system consists of three sections: tube side, membrane and shell side. The steady state two-dimensional material balances were implemented for all three sections. The solvent is fed to the shell side at $z = L$, while the liquid phase is entered the tube side at $z = 0$.

Following Assumptions Were Considered in Modeling:

- Steady state and isothermal conditions;
- Fully developed parabolic velocity profile for the liquid in the hollow fiber;
- The aqueous feed and the dense solvent gas are considered immiscible;
- Reynolds numbers of 2100 and 4000 were considered as the transition limits between laminar and turbulent regimes.

The conservation equations for each species can be expressed as [11]:

$$\frac{\partial(\rho\phi)}{\partial t} + div\left(\rho\bar{u}\phi - \Gamma_\phi grad\phi\right) = S_\phi \tag{1}$$

where ρ is the density of the mixture, ϕ the dependent variable, Γ_ϕ is the velocity vector, ϕ is the appropriate coefficient for variable ϕ, which in the mass fraction equation is calculated as $\Gamma_\phi = \rho D$, D is the mutual diffusion coefficient for mixture and S_ϕ is the source-sink term per unit volume for variable ρ.

The continuity equation for steady state for solute (acetone or ethanol) in the three sections of membrane contactor is obtained using Fick's law of diffusion for estimation of diffusive flux:

$$-D_i\nabla.\left(\nabla C_i\right) + \nabla.\left(C_i V\right) = 0 \tag{2}$$

In a laminar flow, Navier-Stokes equations can be applied for the shell side [11]:

$$\rho\frac{\partial V}{\partial t} - \nabla\cdot\eta(\nabla V + (\nabla V)^T) + \rho(V.\nabla)V + \nabla p = F \tag{3}$$
$$\nabla.V = 0$$

Boundary conditions for the shell side are given as:

$$@ \ z = L, \quad C_{i-shell} = 0 \tag{4}$$

$$@ \ r = r_3, \quad \frac{\partial C_{i-shell}}{\partial r} = 0 \ (\text{insulation}) \tag{5}$$

$$@ \ r = r_2, \quad C_{i-shell} = C_{i-membrane} \tag{6}$$

Boundary conditions for membrane are given as:

$$@ \ r = r_2, \quad C_{i-membrane} = C_{i-shell} \tag{7}$$

$$@ \ r = r_1, \quad C_{i-membrane} = C_{i-tube} \bullet m \tag{8}$$

where m is the physical solubility of the liquid feed in the dense gas.

The velocity distribution in the tube side is assumed to follow Newtonian laminar flow [11]:

$$V_{Z-tube} = 2u\left[1 - \left(\frac{r}{r_1}\right)^2\right] \tag{9}$$

where u is average velocity in the tube side.
Boundary conditions for the tube side are given as:

$$@ \ z = 0, \quad C_{i-tube} = C_{i-inlet} \tag{10}$$

$$@ \ r = r_1, \quad C_{i-tube} = C_{i-membrane}/m \tag{11}$$

$$@ \ r = 0, \quad \frac{\partial C_{i-tube}}{\partial r} = 0 \ (\text{symmetry}) \tag{12}$$

Numerical Solution of Equations: The mass transfer equations related to the tube, membrane and shell side of the contactor along with the boundary conditions were solved using COMSOL Multiphysics software. The latter uses finite element method (FEM) for the numerical solutions of differential equations. The finite element analysis is combined with adaptive meshing and error control using UMFPACK solver. This solver is suited for solving stiff and non-stiff non-linear boundary value problems. The applicability, robustness and accuracy of this model have been verified in previous work [12]. An IBM-PC-Pentium4 (CPU speed is 2800 MHz) was used to solve the set of equations. The computational time for solving the set of equations was about 20 minutes. Parameters and physical constants for numerical simulations were taken from literature [13-17].

RESULTS AND DISCUSSION

Validation of the Mass Transfer Model: The amounts of ethanol and acetone extraction in the membrane contactor were calculated using the simulation developed in this work and were compared with the experimental data reported by Bothun *et al.* [10]. Tables 1 and 2 indicate the calculated and experimental results as functions of the liquid feed flow rate (F) and the solvent/feed molar ratio (S/F).

As it can be seen, the extraction of acetone is higher than ethanol. This is mainly because of the higher hydrophobicity of acetone, i.e. it wets the polypropylene membrane and diffuses into the membrane pores much better than ethanol. It is also well recognized by the model and as it is seen, the model predictions well match the experimental data. Meanwhile, comparing the extraction percentages calculated for ethanol and acetone, the model

Table 1: Experimental and simulated (this work) data for the extraction of ethanol from an aqueous solution using the single-fiber porocritical extraction system (P = 69 bar; T = 298 K; feed solution concentration = 10% w/w)

F (mL/min)	S/F	Extraction (EXP) (%)	Extraction (MOD) (%)	Error (%)
0.15	3	15.2	16.04	5.5
0.25	3	10.4	11.01	5.9
0.50	3	4.7	5.53	17.6
1.00	3	9.9	5.21	47.3
0.10	10	31.9	32.55	2.0

Table 2: Experimental and simulated (this work) data for the extraction of acetone from an aqueous solution using the single-fiber porocritical extraction system (P = 69 bar; T = 298 K; feed solution concentration = 10% w/w)

F (mL/min)	S/F	Extraction (EXP) (%)	Extraction (MOD) (%)	Error (%)
0.15	3	96.1	98.03	2
0.25	3	89.6	87.61	2.2
0.50	3	68.9	67.04	2.7
1.00	3	67.9	65.63	3.3

predictions are found of better accuracy for the acetone extraction. This might be attributed to two aspects; better prediction of transport properties for acetone and better estimation of the vapor-liquid equilibrium for the ternary acetone-CO_2-water system.

The higher accuracy of the model was obtained at lower values of the liquid flow rates (F), as well as lower solvent flow rates (S); the S/F ratio remains constant (S/F = 3) for most of the experimental measurements [4]. The comparisons show an average deviation of 15.6% and 2.5% with the experimental data for ethanol and acetone,

respectively. The results also show that the current mass transfer model is more accurate than the similar model developed by Estay *et al*. [4]. The latter model, which was based on resistances-in-series, shows an average deviation of 36.3% and 6.7% with the experimental data for ethanol and acetone, respectively.

Influence of Hydrophobicity/hydrophilicity of the Membrane: The influence of the membrane hydrophobicity on the extraction of solute was studied using the developed mass transfer model. In a hydrophobic membrane, the aqueous solution does not wet the membrane pores. In this case, the membrane pores are filled with the hydrophobic extraction solvent. On the other hand, for a hydrophilic membrane, however, the pores are filled with the aqueous phase [4]. Generally, in gas-liquid membrane contactors, it is preferred that the gas phase fills the membrane pores because diffusivity in the gas phase is higher than liquid phase and can increase the mass transfer rate of species.

Figs. 3 and 4 present simulated extractions of acetone and ethanol, respectively. These values were obtained by considering either a completely hydrophobic or a hydrophilic membrane where the aqueous solution is circulated within the tube side. The results of simulations show that the hydrophobicity of the membrane is favorable for the extraction of acetone. This observation could be explained by considering that in the case of using a hydrophilic membrane, the mass transfer of acetone is mainly controlled by resistances in the aqueous phase, as well as the diffusion of this compound through the stagnant liquid within the porosity.
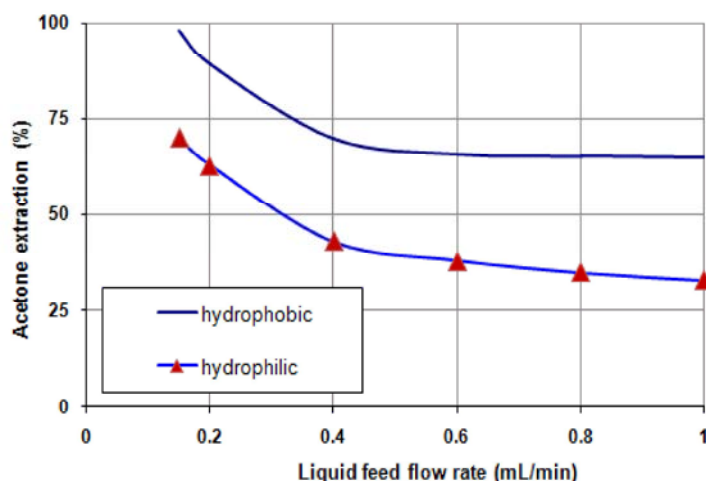

Fig. 3: Extraction of acetone from an aqueous solution (10% w/w) vs the liquid flow rate for hydrophobic/hydrophilic membranes (molar flow ratio S/F = 3; P = 6.9 MPa; T = 298 K)
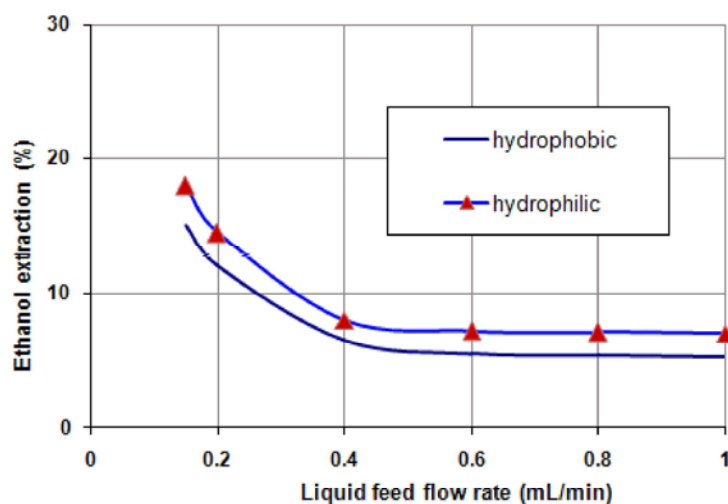
Fig. 4: Extraction of ethanol from an aqueous solution (10% w/w) vs the liquid flow rate for hydrophobic/hydrophilic membranes (molar flow ratio $S/F = 3$; $P = 6.9$ MPa; $T = 298$ K)
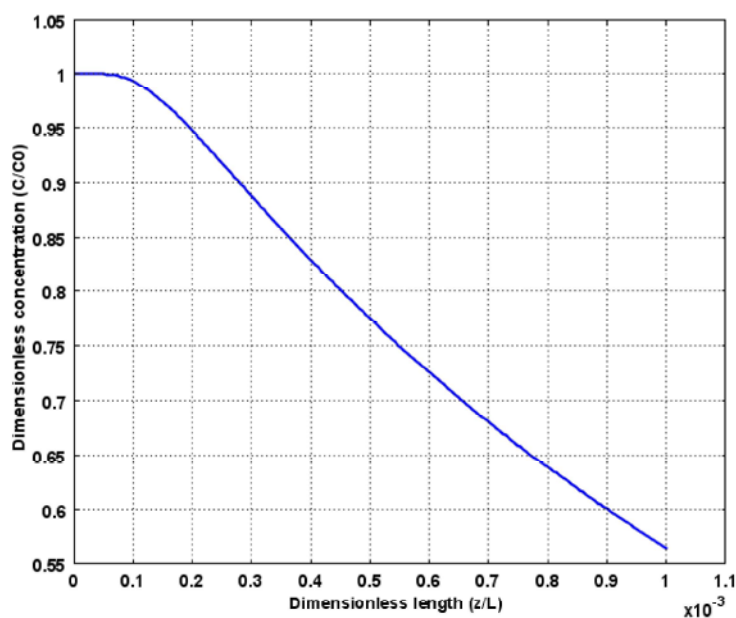

Fig. 5: Axial distribution of acetone concentration (C/C_0) in the contactor (Molar flow ratio $S/F = 3$; $P = 6.9$ MPa; $T = 298$ K; Liquid flow rate = 1 mL/min; Solvent flow rate = 3 mL/min)

Consequently, when a hydrophilic membrane is used, the flux of acetone through the membrane is significantly lower than that for a hydrophobic membrane. Meanwhile, the flux of acetone extraction decreases with the aqueous feed flow rate for both cases of hydrophilic and hydrophobic membranes apparently due to lower contact times attained where the residence time of the phases decreases.

For ethanol extraction, however, because of the hydrophilic nature of ethanol, the mass transfer is mainly controlled by the resistance in the boundary layer of the dense gas solvent. Therefore, in this case, penetration of the aqueous phase into the porosity of a hydrophilic membrane will not significantly lower the permeation behavior of the solute through the membrane and thus the flux of ethanol extraction is higher with hydrophilic membranes [4].

Distribution of the Solute Concentration in the Contactor: Fig. 5 presents the distribution of acetone concentration in the tube side of the membrane contactor. The liquid feed enters from one side of the contactor
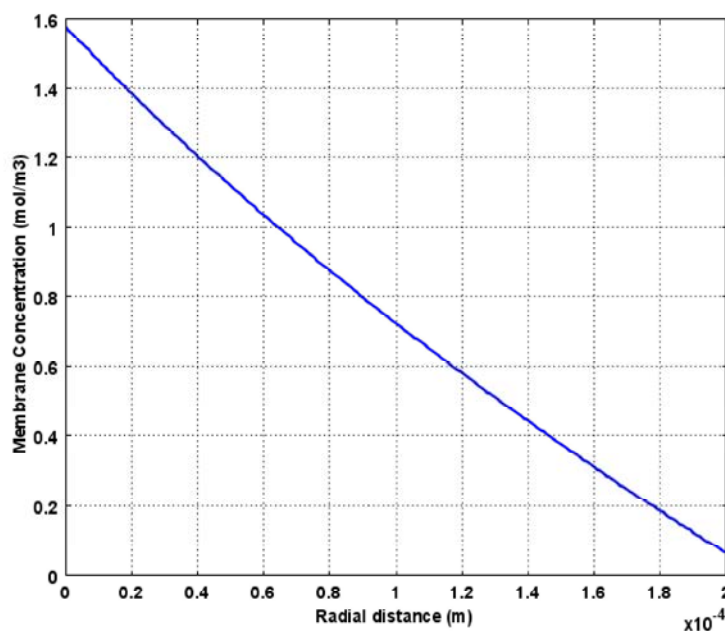
Fig. 6: Radial distribution of acetone concentration in the membrane (Molar flow ratio S/F = 3; P = 6.9 MPa; T = 298 K; Liquid flow rate = 1 mL/min; Solvent flow rate = 3 mL/min)
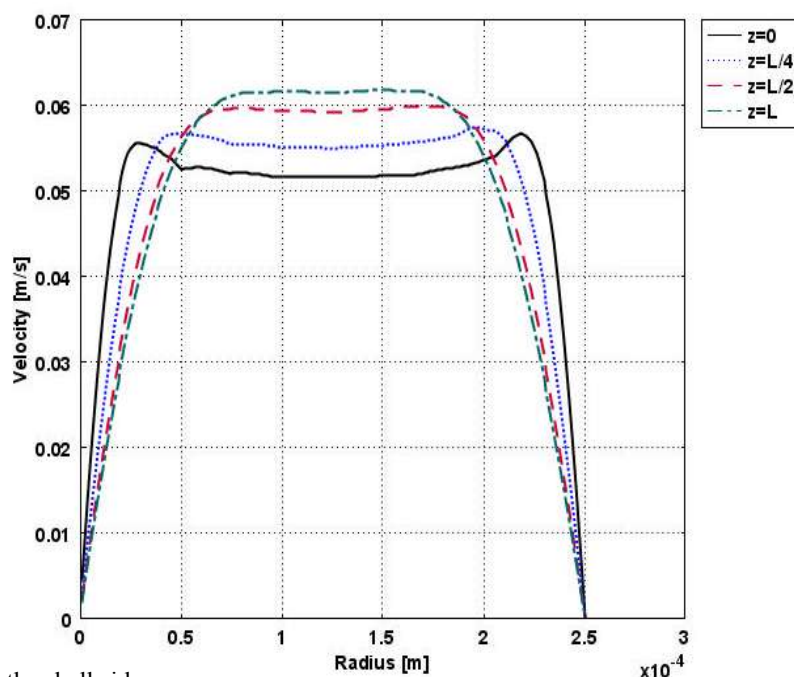

Fig. 7: Velocity profile in the shell side.

(z = 0) where the concentration of acetone is the highest (C_0), whereas the solvent enters from the other side (z = L) where the concentration of acetone is assumed to be zero. As the acetone flows through the tube side, it diffuses to the membrane pores due to the concentration gradient and then becomes extracted into the receiving phase, i.e. the moving solvent.

Fig. 6 also presents concentration distribution of acetone in the membrane. Fig. 6 reveals that concentration distribution inside the membrane is linear. This could be attributed to this fact that Fick's law of diffusion is predominant in this region, i.e. only diffusion mechanism is considered in the membrane which results in a linear concentration profile.

535

Velocity Profile in the Shell Side: The velocity profile in the membrane contactor is shown in Fig. 7, in which the dense solvent (near-critical CO_2) flows. The velocity profile in the shell side was determined by solving Navier-Stokes equations. As it can be seen from Fig. 7, the velocity profile is almost parabolic with a mean velocity which increases with the membrane length because of continuous fluid permeation. Fig. 7 also reveals that at the inlet regions in the solvent (shell) side, the velocity is not developed. After a short distance from the inlet, the velocity profile is fully developed (see Fig. 7). As observed, the model considers the entry effects on the hydrodynamics of fluid flow in the shell side.

CONCLUSIONS

A 2D mass transfer model was developed to study the removal of organic compounds from aqueous solutions by means of hollow-fiber membrane contactors. The model predicts the steady state concentration gradients of the solute in the contactor geometry by solving the conservation equations. The model was developed considering a hydrophobic membrane which is not wetted by the aqueous feed solution. Both axial and radial diffusions within the tube, membrane and shell sides of the contactor were considered. The predictions of the mass transfer model were validated by comparing the results of extractions for ethanol and acetone from aqueous solutions with similar experimental data in the literature.

The simulation results well predicted the higher extraction values for acetone in comparison with those for ethanol where a hydrophobic membrane is used. The results also indicated that the extraction of solute increased with decreasing the liquid velocity in the tube side. The model performed superior, in comparison with similar models, in terms of accuracy as well as being independent of the experimental results.

ACKNOWLEDGEMENT

Nomenclature:

C	concentration, mol/m³
C_{outlet}	outlet concentration of solute in the tube side, mol/m³
C_{intlet}	inlet concentration of solute in the tube side, mol/m³
$C_{i\text{-}tube}$	concentration of solute in the tube side, mol/m³
$C_{i\text{-}shell}$	concentration of solute in the shell side, mol/m³
$C_{i\text{-}membrane}$	concentration of solute in the membrane, mol/m³
D	diffusion coefficient, m²/s
$D_{i\text{-}shell}$	diffusion coefficient of solute in the shell, m²/s
$D_{i\text{-}tube}$	diffusion coefficient of solute in the tube, m²/s
$D_{i\text{-}membrane}$	diffusion coefficient of solute in the membrane, m²/s
F	liquid feed flow, m³/s
L	length of the fiber, m
m	physical solubility
n	number of fibers
P	pressure, Pa
r	radial coordinate, m
r_1	inner tube radius, m
r_2	outer tube radius, m
r_3	inner shell radius, m
R_i	overall reaction rate of any species, mol/m³.s
S	solvent flow rate, m³/s
T	temperature, K
u	average velocity, m/s
V	velocity in the module, m/s
$V_{z\text{-}tube}$	z-velocity in the tube, m/s
z	axial coordinate, m

Greek symbols

ε	membrane porosity
η	viscosity (kg/m.s)
ρ	density (kg/m³)

Abbreviations

EXP	experimental
FEM	finite element method
HFMC	hollow-fiber membrane contactor
MOD	modeling
SCF	supercritical fluid
SFE	supercritical fluid extraction
2D	two dimensional

REFERENCES

1. Afrane, G. And E.H. Chimowitz, 1996. Experimental investigation of a new supercritical fluid-inorganic membrane separation process. J. Membr Sci., 116(2): 293-299.

2. Birtigh, A.A., 1995. Regeneration der Fluidphase bei der Gas extraktion. Technical University of Hamburg, Hamburg.

3. Chiu, Y.W. and C.S. Tan, 2001. Regeneration of supercritical carbon dioxide by membrane at near critical conditions. J. Supercrit. Fluids, 21(1): 81-89.

4. Estay, H., S. Bocquet, J. Romero, J. Sanchez, G.M. Rios and F. Valenzuela, 2007. Modeling and simulation of mass transfer in near-critical extraction using a hollow fiber membrane contactor. Chem. Eng. Sci., 62(21): 5794-5808.

5. Sims, M., E. McGovern and J.R. Robinson, 1998. In Continuous pilot extraction of natural products from liquids with near critical fluids, Porocritical fluid extraction application, Nice, France, 1998; Nice, France.

6. Sarrade, S., C. Guizard and G.M. Rios, 2002. Membrane technology and supercritical fluids: chemical engineering for coupled processes. Desalination, 144(1-3): 137-142.

7. Sarrade, S., G.M. Rios and M. Carlés, 1996. Nanofiltration membrane behavior in a supercritical medium. J. Membr Sci., 114(1): 81-91.

8. Sartorelli, L. and G. Brunner, 2000. In Separation of extracts from supercritical carbon dioxide by means of membranes, International Symposium on Supercritical Fluids, Atlanta, USA, 2000; Atlanta, USA.

9. Sims, M., 1998. Porocritical fluid extraction from liquids using near-critical fluids. Membr. Technol., (97): 11-12.

10. Bothun, G.D., B.L. Knutson, H.J. Strobel, S.E. Nokes, E.A. Brignole and S. Díaz, 2003. Compressed solvents for the extraction of fermentation products within a hollow fiber membrane contactor. J. Supercrit. Fluids, 25(2): 119-134.

11. Bird, R.B., W.E. Stewart and E.N. Lightfoot, 2002. Transport Phenomena. 2nd edition, John Wiley and Sons: New York.

12. Shirazian, S., A. Moghadassi and S. Moradi, 2009. Numerical Simulation of Mass Transfer in Gas-Liquid Hollow Fiber Membrane Contactors for Laminar Flow Conditions. Simulation Modelling Practice and Theory, 17(4): 708-718.

13. Reid, R., J. Prauznit and T. Sherwood, 1977. The Properties of Gases and Liquids. third ed.; McGraw-Hill Inc: New York.

14. Catchpole, O.J. and M.B. King, 1994. Measurement and Correlation of Binary Diffusion Coefficients in Near Critical Fluids. Ind. Eng. Chem. Res., 33(7): 1828-1837.

15. Funazukuri, T., Y. Ishiwata and N. Wakao, 1992. Predictive correlation for binary diffusion coefficients in dense carbon dioxide. AIChE J., 38(11): 1761-1768.

16. Hirohama, S., T. Takatsuka, S. Miyamoto and T. Muto, 1993. Measurement and Correlation of Phase Equilibria for the Carbon Dioxide-Ethanol-Water System. J. Chem. Eng. J., 26(4): 408-415.

17. Adrian, T., M. Wendland, H. Hasse and G. Maurer, 1998. High-pressure multiphase behaviour of ternary systems carbon dioxide-water-polar solvent: review and modeling with the Peng-Robinson equation of state. J. Supercrit. Fluids, 12(3): 185-221.